

# A clinically viable approach to restoring visual function using optogenetic gene therapy

Boyuan Yan,<sup>1,7</sup> Suresh Viswanathan,<sup>2</sup> Scott E. Brodie,<sup>3</sup> Wen-Tao Deng,<sup>4</sup> Kirsten E. Coleman,<sup>5</sup> William W. Hauswirth,<sup>6,7</sup> and Sheila Nirenberg<sup>1,7</sup>

<sup>1</sup>Department of Physiology and Biophysics, Weill Cornell Medicine, New York, NY 10065, USA; <sup>2</sup>Department of Biological and Vision Sciences, College of Optometry, State University of New York, New York, NY 10036, USA; <sup>3</sup>Department of Ophthalmology, NYU Langone Health, New York, NY 10017, USA; <sup>4</sup>Department of Ophthalmology and Visual Sciences, School of Medicine, West Virginia University, Morgantown, WV 26506, USA; <sup>5</sup>Powel Gene Therapy Center Toxicology Core, University of Florida, Gainesville, FL 32610, USA; <sup>6</sup>Department of Ophthalmology, College of Medicine, University of Florida, Gainesville, FL 32603, USA; <sup>7</sup>Bionic Sight, Inc., New York, NY 10065, USA

**Optogenetic gene therapies offer a promising strategy for restoring vision to patients with retinal degenerative diseases, such as retinitis pigmentosa (RP). Several clinical trials have begun in this area using different vectors and optogenetic proteins (Clinical Identifiers: NCT02556736, NCT03326336, NCT04945772, and NCT04278131). Here we present preclinical efficacy and safety data for the NCT04278131 trial, which uses an AAV2 vector and Chronos as the optogenetic protein. Efficacy was assessed in mice in a dose-dependent manner using electroretinograms (ERGs). Safety was assessed in rats, nonhuman primates, and mice, using several tests, including immunohistochemical analyses and cell counts (rats), electroretinograms (nonhuman primates), and ocular toxicology assays (mice). The results showed that Chronos-expressing vectors were efficacious over a broad range of vector doses and stimulating light intensities, and were well tolerated: no test article-related findings were observed in the anatomical and electrophysiological assays performed.**

## INTRODUCTION

Retinitis pigmentosa (RP) is a large group of inherited retinal disorders in which progressive degeneration of photoreceptors leads to vision loss. The clinical manifestations of affected individuals present first as night blindness, followed by reduction of peripheral vision and, eventually, loss of central vision.

Current treatments for patients with RP are limited. There is some evidence to suggest that vitamin A and fish oil supplements may slow vision loss in some patients with early disease,<sup>1</sup> but they are not able to reverse the disease. For a subset of patients whose retinal degeneration is caused by a mutation in the RPE65 gene, targeted gene therapy is now possible<sup>2–5</sup> and is currently being used to treat patients (reviewed in Maguire et al.<sup>6</sup>). However, because RP is a genetically heterogeneous disease, with more than 100 different genes or loci that lead to the common endpoint of vision loss (<https://web.sph.uth.edu/retnet/sum-dis.htm#B-diseases>), this particular gene therapy does not apply to the majority of RP patients.

New gene therapies that employ optogenetics, however, are opening up new options for patients with RP. With optogenetics, it is possible to treat the disease in a way that is independent of the underlying gene defect, allowing a much broader range of patients to obtain benefit. Briefly, one of the main versions of the approach is as follows: an optogenetic protein, such as a channelrhodopsin (ChR), is delivered to the retina's output cells, the ganglion cells,<sup>7–12</sup> although bipolar cells have also been utilized.<sup>13–16</sup> The ChR is then light-activated, which causes the ganglion cells to fire and send neural signals through the optic nerve to the brain. Different investigators are using different strategies to perform the light activation, with some incorporating externally worn goggles that contain an embedded light-delivery device (reviewed in Barrett et al.<sup>17</sup>).<sup>9,18,19</sup> Nirenberg and Pandarinath<sup>9</sup> take the approach a step further, using a light-delivery device that sends signals in the retina's neural code, causing the ganglion cell firing to closely mimic that of the normal retina. This combination of optogenetic gene therapy and neurally coded stimulation has the potential to offer significantly better and more detailed vision restoration to patients with advanced stage blindness due to RP.

The initial optogenetic therapies utilized channelrhodopsin-2 (ChR2) as the optogenetic protein,<sup>7,8,13,14</sup> as this was one of the first optogenetic proteins discovered (reviewed in Mattis et al.<sup>20</sup>). While highly promising as a concept, this particular protein had limitations as a therapy because it (1) requires very bright light to activate it, and (2) its excitation wavelength is short (near blue, with peak excitation at 460 nm<sup>21</sup>), both of which increase its risk of producing phototoxic effects.

In the past decade, more optogenetic proteins<sup>22–25</sup> and light-activated photoswitches (Gaub et al.<sup>26</sup>; reviewed in Tochitsky et al.<sup>27</sup>; Berry et al.<sup>28</sup>) have been developed, providing an increasing arsenal of tools

Received 2 October 2021; accepted 4 May 2023;  
<https://doi.org/10.1016/j.omtm.2023.05.005>.

**Correspondence:** Sheila Nirenberg, Department of Physiology and Biophysics, Weill Cornell Medicine, New York, NY 10065, USA.

**E-mail:** [shn2010@med.cornell.edu](mailto:shn2010@med.cornell.edu)

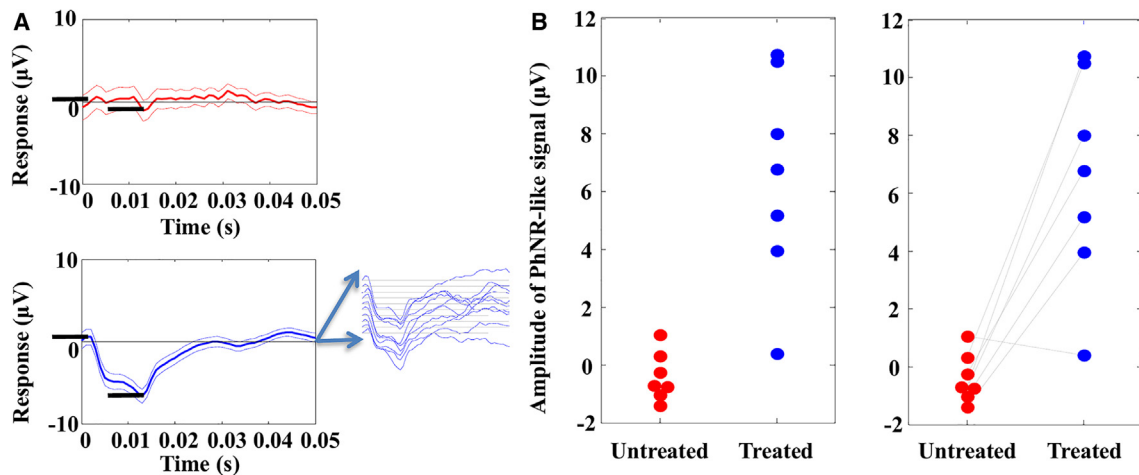


**Figure 1. BS01 produces robust ERG responses in rd1 mice**

(A) Raw ERG responses (mean  $\pm$  SEM) from an untreated eye (top, red) and a BS01-treated eye (bottom, blue) from the same animal. Horizontal black lines on each plot indicate the locations of the stimulus-induced photovoltaic effects, i.e., small upward and downward electrical transients at stimulus onset and offset. The Chronos activated ERG response lies between these transients. Note that the photovoltaic transients are visible in both the untreated and treated eye, but the deep dip in the ERG, corresponding to the PhNR, is only present in the treated eye (bottom panel). To the right of the bottom panel are a set of traces from separate non-overlapping epochs in the ERG, indicating consistency over the entire acquisition period. (B) ERG responses for all animals. For each eye in each animal, the response was quantified by the size of the PhNR-like wave (the ERG component that corresponds to the ganglion cell response), measured as the difference between the voltage at time zero and the average voltage during the last half of the stimulation period, just prior to the photovoltaic transient. A clear PhNR-like wave was observed in six of the seven animals examined. The size of the wave was significant both at a group level ( $p < 0.001$ , unpaired  $t$  test), and at the level of the individual animals ( $p < 0.004$ , paired  $t$  test, comparing, for each animal, its treated eye with its untreated counterpart, shown on the right). Some variance in the responses is expected due to injection variance in a small target (mouse eye). Outcomes were measured 10 weeks after vector injection. Light stimulation was  $0.06 \text{ mW/mm}^2$ ,  $505 \text{ nm}$ , and  $11.2 \text{ ms}$  long.

to move the field forward. As a result, there are now several clinical trials using optogenetics as a therapeutic: ClinicalTrial.gov identifier: NCT02556736<sup>29</sup> (Retrosense/Allergan/AbbVie), ClinicalTrial.gov identifier: NCT03326336<sup>30</sup> (GenSight Biologics), ClinicalTrial.gov identifier: NCT04945772<sup>31</sup> (Nanoscope Therapeutics Inc.), and ClinicalTrial.gov identifier: NCT04278131<sup>32</sup> (Bionic Sight Inc.). In this paper, we present the main preclinical studies underlying NCT04278131, the Bionic Sight trial. The vector used in this trial, referred to as BS01 (AAV2-CAG-ChronosFP-WPRE), utilizes Chronos as the optogenetic protein.<sup>25</sup> It was chosen because Chronos was reported to be  $>10$ -fold more sensitive to light than Chr2,<sup>25</sup> and has a longer excitation wavelength (peak excitation is  $500 \text{ nm}$ ), which together bring a significant reduction in potential phototoxicity.<sup>33,34</sup> In the studies shown here and in NCT04278131, Chronos is fused to green fluorescent protein (GFP) to produce a protein called ChronosFP. Here we present data in animal models on both the efficacy and safety of ChronosFP-expressing vectors. These data can later be compared with the results of the clinical trial. Reporting preclinical data is highly valuable, as it provides insight into what measures in animal studies were important and had predictive value when the treatment was subsequently applied to humans.

## RESULTS

### BS01 produced clear electroretinogram responses in blind mice

To test the efficacy, photopic electroretinograms (ERGs) were performed in adult rd1 mice, a widely used model for retinal degenerative disease<sup>13,35–38</sup>; rd1 has an earlier onset of retinal degeneration than

the rd10 model.<sup>39</sup> Briefly, the photopic ERG response in normal animals is composed of three components: the a-wave, which corresponds to photoreceptor signaling; the b-wave, which corresponds to bipolar cell signaling; and the photopic negative response (PhNR), which corresponds to ganglion cell signaling.<sup>40</sup> In rd1 animals, which lose photoreceptor outer segments by 8 weeks of age,<sup>9,36</sup> none of these components are present.<sup>41</sup> If these animals are engineered to express an optogenetic protein in their ganglion cells, the prediction is that a PhNR-like wave would emerge, reflecting the newly created optogenetic activity of the ganglion cells. We thus conducted ERGs on BS01-treated eyes to test for the presence of a newly created PhNR-like wave.

Seven rd1 mice received BS01 by intravitreal injection into one eye at a dose of  $5 \times 10^8 \text{ vg/eye}$ , which is comparable to a dose of  $5 \times 10^{11} \text{ vg/eye}$  in humans<sup>42–44</sup> (see also Table S1). This dose was chosen as a starting point, aiming to be comparable to one of the first intravitreal doses of an AAV-type vector in human trials that was available at the time (NCT02416622<sup>45</sup>); this is also comparable to studies in animal models.<sup>10,16</sup> Outcomes were measured at 10 weeks post injection, when the ChronosFP expression was expected to have peaked. The untreated eye of each animal served as the control. The results showed that six of the seven animals produced clear and reliable light-evoked ERG responses (PhNR-like waves) in their treated eyes; this is in contrast to the ERGs produced by the untreated eyes of the same rd1 animals, which showed flat ERG responses (Figure 1). The results were significant at both a group level ( $p < 0.001$ , unpaired  $t$  test comparing the

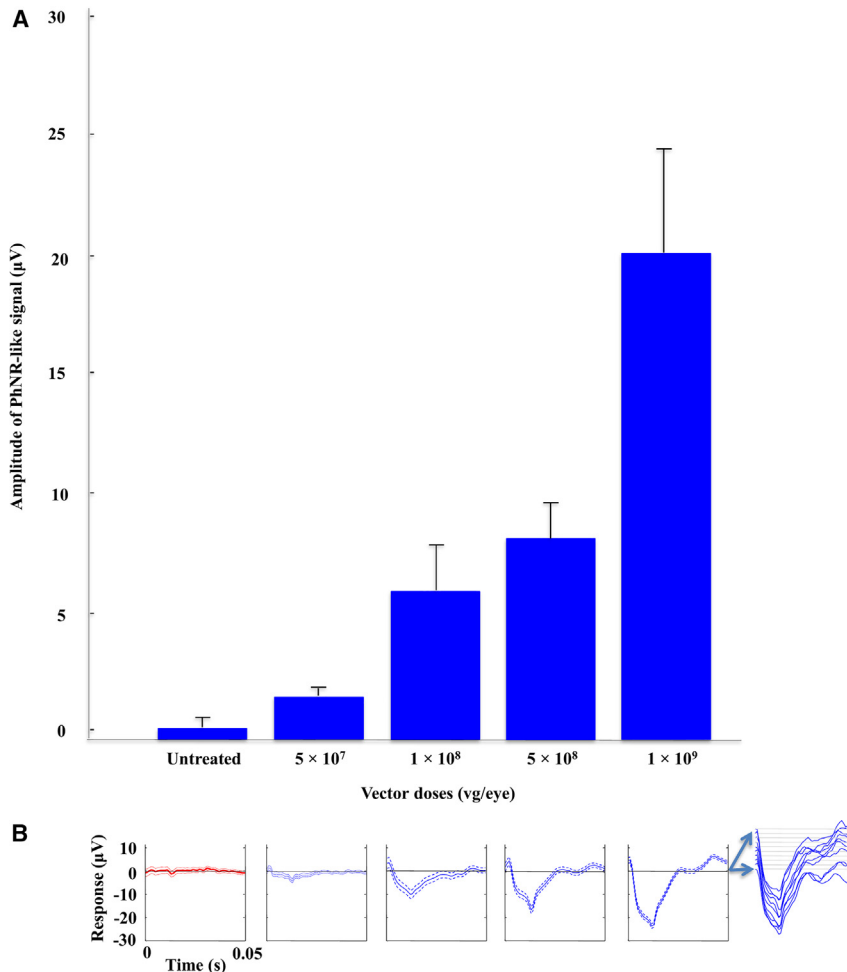


**Figure 2. Assessing ERG responses in rd1 mice over a 20-fold dose range**

(A) ERG responses to light stimulation from animals that were treated with BS01. Five groups are shown: untreated eyes ( $n = 7$ ), eyes treated with a dose of  $5 \times 10^7$  vg/eye ( $n = 7$ ), eyes treated with a dose of  $1 \times 10^8$  vg/eye ( $n = 3$ ), eyes treated with a dose of  $5 \times 10^8$  vg/eye ( $n = 12$ ), and eyes treated with a dose of  $1 \times 10^9$  vg/eye ( $n = 11$ ). The mean response amplitude for each dose group was statistically significantly different from that of the control ( $p < 0.01$ , Student's *t* test), and, as expected, response amplitude increased with increasing dose. (B) Raw ERG responses (mean  $\pm$  SEM) from each of the five groups. The response for each eye was quantified by the size of the PhNR-like wave. All injections were performed 10–15 weeks prior to recording. Light stimulation was  $0.06 \text{ mW/mm}^2$ , 505 nm.

magnitude of the ERG signal from treated eyes with those from the untreated eyes), and at an individual level ( $p < 0.004$ , paired *t* test, comparing, for each animal, its treated eye with its untreated counterpart). The ChronosFP-induced PhNR has a short latency; this occurs because the ganglion cells are being activated directly, rather than through the photoreceptor-to-bipolar cells pathway.

#### The magnitude of the ERG response was dose dependent, both with respect to viral dose and light dose

Following the experiments shown in Figure 1, the effectiveness of BS01 over a broader range of doses was explored, from 10-fold lower ( $5 \times 10^7$  vg/eye) to 2-fold higher ( $1 \times 10^9$  vg/eye). Figure 2 shows the results over this 20-fold range; all dose levels were statistically significantly different from the control group ( $p < 0.01$ , Student's *t* test, comparing each dose group with the untreated group), and, as expected, the amplitudes of the responses increased with increasing vector dose.

Given the robust PhNR-like responses at the higher vector doses, we also explored whether the intensity of the light stimulation could be reduced and still produce a light response. Specifically, using the

two highest doses, we assessed how far the light level could be dropped while still maintaining a PhNR-like amplitude that was significantly above the control level. The results showed that the light level required for a vector dose of  $1 \times 10^9$  vg/eye could be reduced by approximately a factor of 10 (Figure 3). For the next highest dose,  $5 \times 10^8$  vg/eye, the light level could be reduced by a factor of 6 ( $p < 0.01$ , Student's *t* test). The effects on lower vector doses were not tested, since there was little room for adjustment. These results served to narrow the range of light levels needed for testing in a clinical trial, reducing the burden of exploration with patients. We emphasize also that the controls in this study (see Figure 2), which were blind, untreated eyes, always received the maximal light intensity ( $0.06 \text{ mW/mm}^2$ ). Thus,

without the vector treatment, blind eyes showed no response even to the brightest light in this regimen, whereas with BS01 treatment, the eyes responded with robust ERG signals even when light levels were dropped substantially. We also note that light levels can likely be dropped further when perceptual studies are performed with human subjects, since ERG responses are well known to be less sensitive than perceptual ones.<sup>46</sup>

#### Assessing safety

The ERG responses in rd1 mice demonstrated that BS01 is effective in producing light responses in blind animals. To assess the vector's safety, studies were performed in rats, nonhuman primates, and mice, using several tests, including immunohistochemical analyses and cell counts (rats), ERGs (nonhuman primates), and ocular tolerance/toxicology assays (mice).

#### Assessing safety using immunohistochemical analyses and cell counts in rats

Similar to the rd1 mouse line and human patients with RP, S334ter-3 rats have an inherited retinal degenerative disease that leads to severe

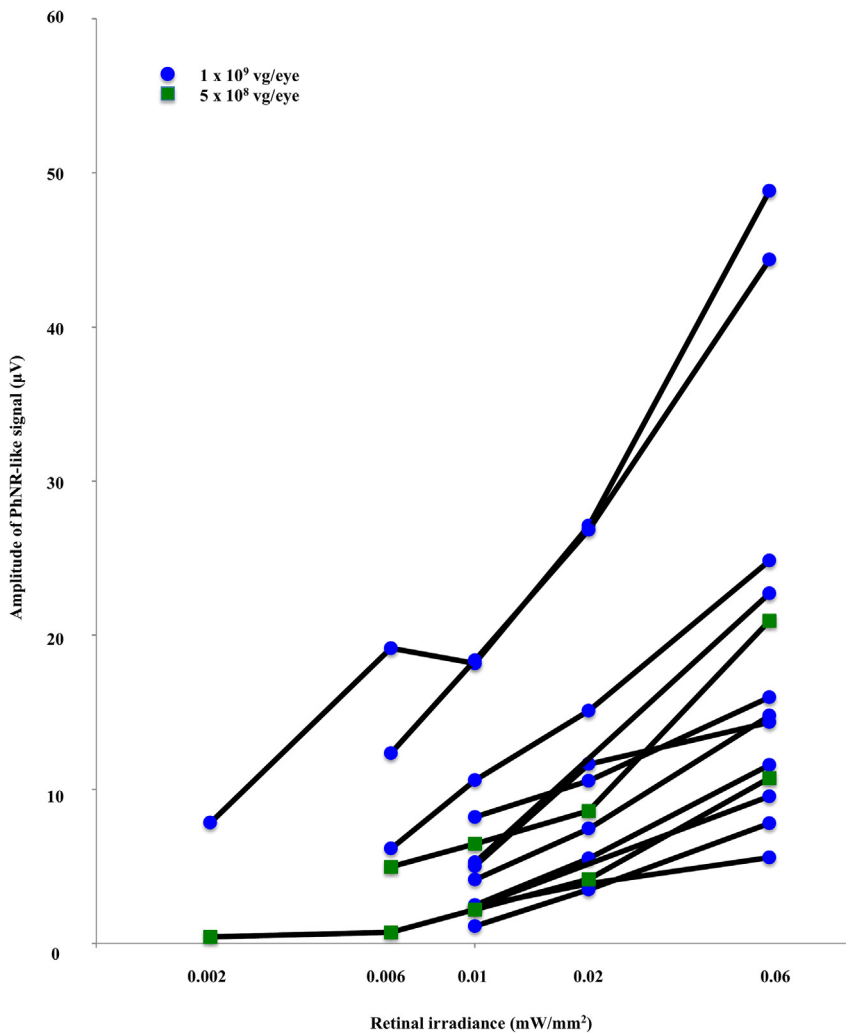


**Figure 3. Assessing ERG responses in BS01-treated rd1 mice to lower light levels**

For animals treated with the two highest doses,  $1 \times 10^9$  vg/eye and  $5 \times 10^8$  vg/eye, light levels could be substantially reduced from the level used in Figures 1 and 2 ( $0.06 \text{ mW/mm}^2$ ) and still produce ERG responses that were well above baseline (see untreated eyes in Figure 2) ( $p < 0.01$ , Student's t test). All injections were performed 10–15 weeks prior to recording.

the ganglion cell layer. If treatment with BS01 was detrimental to the targeted cells, one would expect a loss of cells in the ganglion cell layer of the treated retinas compared with controls. Ganglion cells were labeled with two markers, one that labels ganglion cells in general (Brn3)<sup>49</sup> and one that labels the ChronosFP-expressing cells specifically (an antibody to GFP). Cell counts were performed 5 months after BS01 injection to allow for cell death, if it occurred, as well as removal of cellular debris.<sup>50</sup> Figure 4 shows the results: there was no statistically significant difference in retinal ganglion cell counts between the low-dose group and the control group 5 months after treatment ( $p > 0.1$ , Student's t test) or between the high-dose group and the control group ( $p > 0.5$ , Student's t test).

The second set of experiments assessed the safety of the vector plus light stimulation. These were divided into two parts. The first focused on testing for the presence of ChronosFP-expressing cells. Since these cells had been made light-sensitive by expressing ChronosFP in them, there was a possibility that light stimulation would damage them, limiting the value of a therapy that required light stimulation. To assess the safety of light-activating ChronosFP-expressing cells, we treated two groups of four animals with BS01, both at  $2.7 \times 10^9$  vg/eye. The animals in one group received light stimulation similar to the exposure expected in a clinical trial with an optogenetic vector (12 2-h sessions of direct stimulation over a period of 8 weeks at  $0.1 \text{ mW/mm}^2$  [see materials and methods]), while the other group of animals received no light stimulation. The retinas were processed 5 months after the light stimulation. The results showed no difference in the number of ChronosFP-expressing cells in the two groups, indicating no loss of ChronosFP-expressing cells as a result of the light exposure (Figures 5A and 5B) ( $p > 0.7$ , Student's t test).

The second part of the study focused on photoreceptors, assessing whether the light stimulation needed to drive ChronosFP in the ganglion cells caused damage to the naturally light-absorbing cells in the retina, the photoreceptors. For these experiments, wild-type (WT), rather than S334ter-3, animals, were used since adult S334ter-3 rats no longer have a photoreceptor layer as a result of their retinal

loss of photoreceptors.<sup>47</sup> Two sets of experiments were performed. The first assessed the safety of the BS01 vector, the second assessed the safety of the BS01 vector combined with the light stimulation needed to activate it.

For the first set, three groups of animals were used: a low-dose group that received  $6.8 \times 10^8$  vg/eye, which corresponds to  $6.7 \times 10^7$  vg/eye in mice,<sup>48</sup> a high-dose group that received  $2.7 \times 10^9$  vg/eye, which corresponds to  $2.6 \times 10^8$  vg/eye in mice, and a control group that contained both vehicle-treated eyes and untreated eyes. Note that there is a wide range of vitreous volumes that have been reported for rat eyes (13–54  $\mu\text{L}$ ).<sup>48</sup> To be conservative with respect to safety, we assumed the largest volume for the rat vitreous (54  $\mu\text{L}$ ) when converting to the mouse equivalent dose (mouse vitreous is 5.3  $\mu\text{L}$ ). Thus, the doses used here may be considerably higher (as much as four times higher) and, therefore, provide an even stronger assessment of the toxicity of BS01 to ganglion cells. For reference, Table S1 provides dose equivalents for different species, including mouse, rat, nonhuman primate, and human. The assay performed was to count the number of cells in

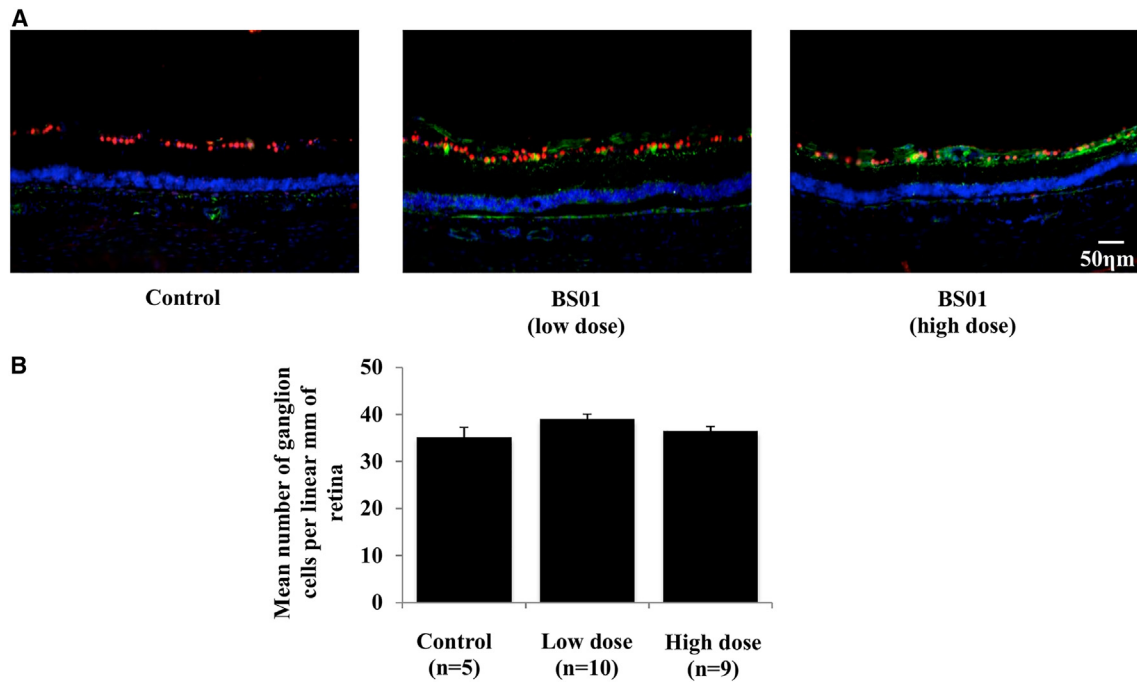


**Figure 4. No loss of retinal ganglion cells in BS01-treated retinas compared with untreated retinas**

(A) From left to right, S334ter-3 rat retinas from control, low-dose BS01-treated, and high-dose BS01-treated eyes. Retinas were labeled with a general marker for retinal ganglion cells (a Brn3a antibody, red), and a marker for ChronosFP (an anti-GFP antibody, green). DAPI was also used as a counterstain (blue). Eyes were sectioned perpendicularly from dorsal to ventral, and Brn3a-positive cell bodies were counted in sections over 650 μm length regions at a 650 μm distance from the edge of optic nerve heads. Scale bar, 50 μm. (B) Mean density of Brn3a-positive cells from control retinas, low-dose BS01-treated retinas, and high-dose BS01-treated retinas. Data are plotted as the number of ganglion cells per linear millimeter of retina (mean ± SEM). No statistically significant difference was observed in retinal ganglion cell counts between the low-dose group and the control group ( $p > 0.1$ , Student's *t* test) or between the high-dose group and the control group ( $p > 0.5$ , Student's *t* test). The low-dose group contained 10 eyes, the high-dose group contained nine eyes, and the control group contained three vehicle-treated eyes and two untreated eyes.

degenerative disease.<sup>47,51</sup> Six WT animals were assessed: In each, one eye received BS01 plus light treatment (12 2.5-h sessions over a period of 6 weeks at 0.1 mW/mm<sup>2</sup>), and the other eye received no treatment. The BS01 dose was  $8.4 \times 10^9$  vg/eye, which corresponds to  $8.2 \times 10^8$  vg/eye in mice. The retinas were removed 6 months post-injection. The results (Figures 5C and 5D) showed no loss of photoreceptors (cones) in the BS01-plus light treated retinas compared with the untreated retinas ( $p > 0.4$ , Student's *t* test). These results are consistent with previous results on light stimulation for optogenetic therapies reported in Yan et al.<sup>34</sup> showing no loss to the photoreceptor layer, which contains both rods and cones, as measured by retinal thickness (outer nuclear layer thickness) and using the same wavelength and light level.

#### Accessing the safety of ChronosFP in nonhuman primates using ERGs

The study in rats assessed tissue integrity using immunohistochemistry and cell count assays. To examine safety electrophysiologically and in a species similar to humans, ERGs were performed on cynomolgus macaques. Three animals (six eyes total) were assessed 7 months after vector administration by intravitreal injection. One animal (both eyes) received BS01 and two animals (both eyes)

received a variant that used the same transgene (ChronosFP) but was packaged using a different AAV2 capsid (the AAV2tYF capsid<sup>52</sup>). The doses fell within the range used in the efficacy study in Figure 2; doses were  $3.7 \times 10^{10}$  vg/eye and  $1.2 \times 10^{11}$  vg/eye, which is equivalent to  $1 \times 10^8$  vg/eye and  $3.2 \times 10^8$  vg/eye in mice<sup>48</sup> (see also Table S1). Four animals (eight eyes total) were untreated and served as controls.

To assess whether ERG responses were adversely affected in treated vs. untreated eyes, we focused on the three standard photopic ERG components: the a- and b-waves, which reflect photoreceptor and bipolar cell responses, respectively, and the PhNR wave, which reflects ganglion cell responses. Seven months after vector injection, intensity/response data were fit to a generalized Naka-Rushton function to derive the saturated amplitude for each wave, the  $V_{max}$ , following reference.<sup>53</sup> As shown in Figure 6, there was no statistically significant reduction in  $V_{max}$  observed for any of the three ERG components as a result of the treatment ( $p > 0.2$ , for all waves, comparing the  $V_{max}$  values in the treated group with those in the untreated group).

The ERG safety experiments shown in Figure 6 show results at a macroscale, i.e., whole retina electrophysiology. In this section, we

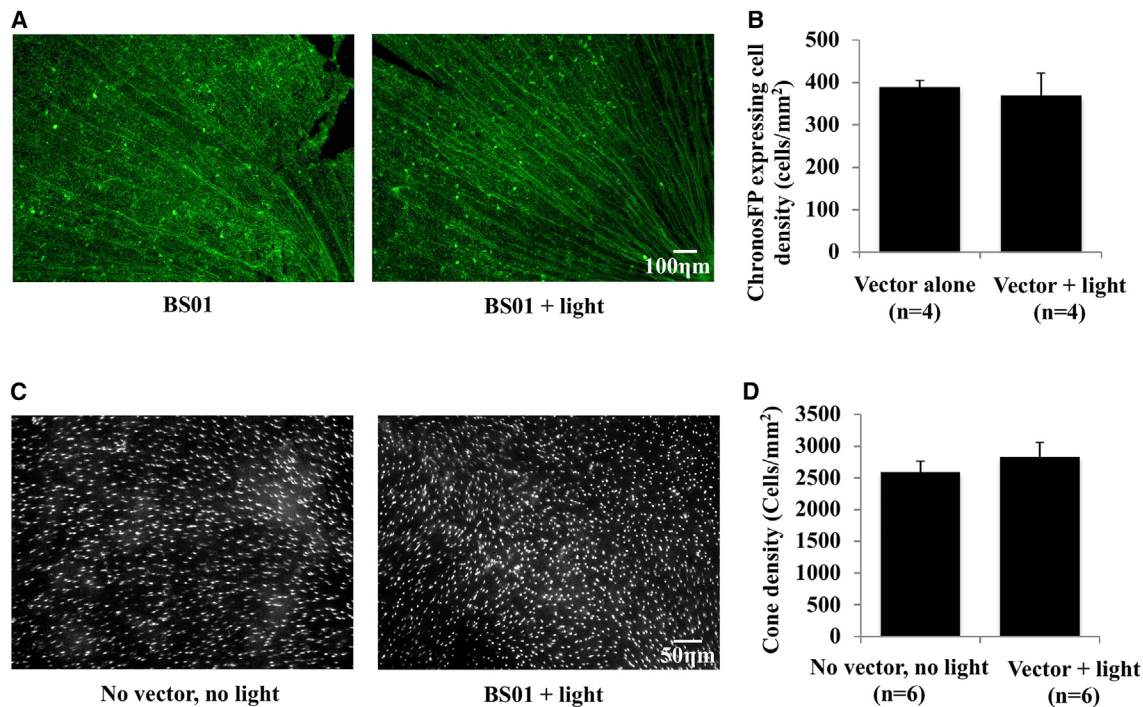


**Figure 5. No loss of ChronosFP-expressing ganglion cells and photoreceptors in retinas treated with both BS01 and light**

(A) Wholemount retinas stained with antibodies to GFP, a marker for ChronosFP. The left panel shows a retina from an eye treated with BS01 5 months before enucleation; this eye did not receive light treatment. The right panel shows a retina treated with BS01 5 months before enucleation; this eye received light treatment consisting of 12 2-h sessions over a period of 8 weeks. Scale bar, 100  $\mu$ m. (B) Comparison of the densities (mean  $\pm$  SEM) of ChronosFP-expressing cells in the BS01-alone group and the BS01-plus-light-treated group; no statistically significant difference between the two groups was observed ( $p > 0.7$ , Student's *t* test). (C) Wholemount retinas stained with a marker for cone photoreceptors (peanut agglutinin [PNA]). The left panel shows a retina from an untreated eye. The right panel shows a retina from an eye that was injected with BS01 6 months before enucleation and received the light treatment in 12 2.5-h sessions over a period of 6 weeks. Scale bar, 50  $\mu$ m. (D) Comparison of the densities (mean  $\pm$  SEM) of cones in the untreated retinas with those in the BS01-plus-light-treated retinas; no statistically significant difference was observed ( $p > 0.4$ , Student's *t* test).

provide additional safety evaluation at the single-cell level. Multi-electrode array (MEA) recordings from excised retinas of cynomolgus macaques that were previously injected with ChronosFP-expressing vectors were evaluated for receptive field size and mean firing rate. The retinas from six eyes (three animals) were treated with an array of ChronosFP-expressing vectors; for these experiments, the capsid was the AAV2 variant AAV2tYF, the promoters were CAMKII, hCACNA1G, and mNefL1.6, and the dose range was from  $2.2 \times 10^{11}$  vg/eye to  $7.6 \times 10^{12}$  vg/eye (equivalent to  $5.8 \times 10^8$  vg/eye to  $2 \times 10^{10}$  vg/eye in mouse). The results showed that the distributions of receptive field sizes and firing rates from the ChronosFP-treated group were not statistically significantly different from those from the untreated group (Figure 7) ( $p > 0.2$ , Kolmogorov-Smirnov test), that is, retinal ganglion cells sampled from eyes that had been injected intravitreally with a ChronosFP-expressing vector showed receptive field sizes and firing rates that were very similar to those from untreated retinas, with the stimuli used to assess firing rates drawn from natural scenes (e.g., trees, landscapes, people walking).

#### Assessing local tolerance in blind mice

Last, we assessed the safety of BS01 in terms of local tolerance. A total of 120 rd1 mice were divided into three groups (40 animals per

group): two dose groups spanning a factor of 10 in dose level ( $4.25 \times 10^8$  vg/eye and  $4.25 \times 10^9$  vg/eye) and a vehicle-alone group. Injections were performed intravitreally to the right eye, and the left eye remained untreated. Each group had two time points, week 4 and week 12 (20 animals at each time point), when animals were euthanized.

Transgene expression in the injected eyes was verified (Figure 8, Table S2). ChronosFP expression, measured by GFP-immunolabeling (magenta), was detected in nerve fiber layer, inner plexiform layer, optic disc, and the extending axons in all animals.

Ophthalmic examinations were performed on weeks 2, 4, 8, and 12 post-injection, and the findings are summarized in Table S3. A slit lamp was used to assess anterior segments including cornea, iris, and lens. An indirect ophthalmoscope was used to assess the posterior segments including vitreous chambers and retinas. Previous phenotypic characterizations of rd1 mice have shown that their eyes have vessel attenuation and pigment patches at an early age.<sup>54,55</sup> Consistent with this, these phenotypes were present at similar frequencies in both the BS01 and vehicle-injected eyes in our study, suggesting that they were not caused by the vector.

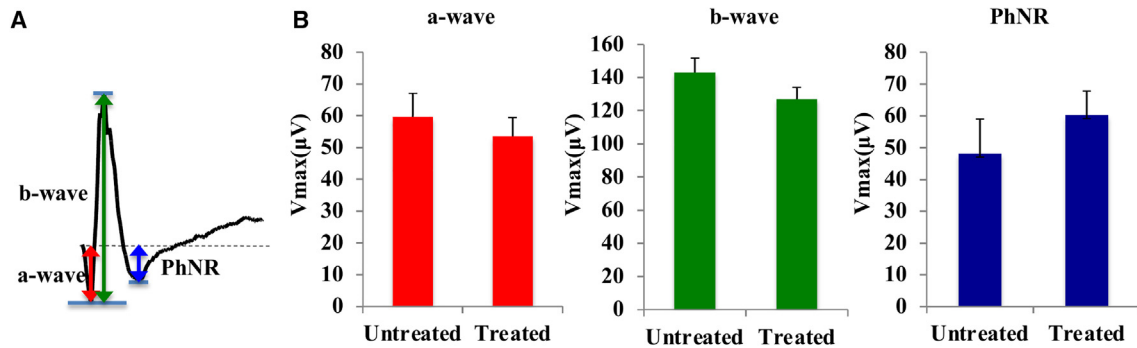


**Figure 6. No statistically significant drop in the amplitude of ERG components between treated and untreated eyes in nonhuman primates**

(A) Representative ERG response to a flash stimulus showing the three main ERG components: the a-wave, the b-wave, and the PhNR. (B) Mean  $V_{max}$  values for the three ERG components in the untreated and treated groups (mean  $\pm$  SEM). No statistically significant reduction in  $V_{max}$  was observed for any of the three components as a result of the treatment ( $p > 0.2$ , Student's *t* test, for all waves, comparing the  $V_{max}$  values in the treated group with those in the untreated group). The ERGs for the treated animals were performed 7 months after vector injection.

In hematoxylin and eosin-stained retinal sections, BS01-related microscopic findings included minimal to slight mononuclear cell infiltrates in the vitreous,<sup>56</sup> where minimal is the lowest level in a 5-level classification (Table S4). By terminal euthanization (week 12), only the lowest (minimal level) mononuclear cell infiltrates were present.

## DISCUSSION

Optogenetic gene therapies offer a potential strategy for restoring sight to patients with retinal degenerative diseases. In this study, we assessed the efficacy and safety of a potential therapeutic AAV2 vector that uses Chronos as the optogenetic protein. Efficacy was assessed in mice in a dose-dependent manner using ERGs, and safety was evaluated in several species using several tests, including immunohistochemical analyses and cell counts (rats), ERGs (nonhuman primates), and ocular toxicology assays (mice). The results showed that Chronos-expressing vectors were efficacious over a broad range of vector doses and stimulating light intensities, and were well tolerated: no test article-related findings were observed in the anatomical and electrophysiological assays performed. These results paved the way for the ongoing clinical trial, ClinicalTrials.gov. NCT04278131.

### Combining optogenetics with neural coding

While optogenetic gene therapy applied to retinal ganglion cells holds great promise for sending visual signals to the brain, we do not expect it to serve as a complete treatment for patients with advanced stage blindness. This is because the retina is an image processing tissue, and optogenetic therapy needs to be combined with a device that performs this processing for the patients. Briefly, when images enter a normal retina, they activate the photoreceptors, which convert the images into electrical signals. The signals are then passed through the retinal circuitry, which extracts features from the images (the building blocks for visual perceptions) and converts the features into a code. The coded signals are then sent from the retinal ganglion cells to the brain. When optogenetic therapy is combined with a neural coding device, it opens the door to producing meaningful percep-

tions (e.g., of faces, objects, and landscapes), as described and demonstrated using the mouse retina in Nirenberg and Pandarinath.<sup>9</sup>

Chronos is a particularly good fit to interface with a neural coding device, because of its fast kinetics. The temporal resolution driven by a channelrhodopsin is largely limited by the off-kinetics of its photocurrent (i.e., the kinetics of current decay after the cessation of light). As one of the fastest channelrhodopsins, Chronos has an off time of 3.6 ms, which is much faster than ChR2 (~10 ms) and ChrimsonR (15.8 ms).<sup>25</sup>

### Light safety with respect to optogenetic therapy

Light safety has been a concern for clinical applications of optogenetics, as early channelrhodopsins required bright light of relatively short wavelengths. However, this problem has been significantly reduced in two ways: (1) by the properties of Chronos: it has significantly higher light sensitivity and a longer peak absorption wavelength (500 nm), and (2) by using a device that delivers neurally coded stimuli. The latter helps because neuronal firing is well known to be sparse (cells fire on average only 5%–10% of the time),<sup>9,34,57,58</sup> so stimulation that follows the neural code keeps the accumulated light exposure low, even when very bright pulses, such as those used in Figures 2 and 3 (0.06 mW/mm<sup>2</sup>), are used.<sup>34</sup>

A previous study<sup>34</sup> assessed exposure limits for various stimulation protocols, following the limits provided by the American National Standards Institute (ANSI 2014).<sup>33</sup> In particular, the study took movies of natural scenes, encoded them into trains of light pulses following Nirenberg and Pandarinath,<sup>9</sup> and assessed the exposure the light produced relative to the ANSI limits. Because of the sparse nature of the neurally coded representation of the movies, the exposure fell well below the ANSI limit, even using 0.06 mW/mm<sup>2</sup> for the pulses, running the movies for 8 h, and including the newer (2014) restriction by ANSI, the Luminance Dose Restriction.<sup>34</sup>

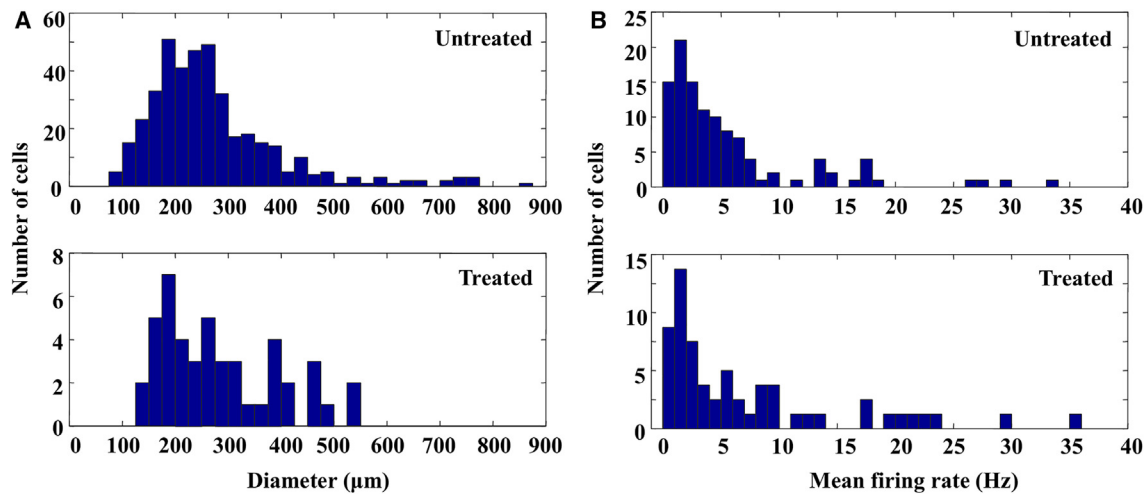


**Figure 7. The distribution of ganglion cell receptive field sizes and firing rates from ChronosFP-expressing retinas was not statistically significantly different from those of untreated retinas**

(A) Histogram of receptive field sizes from untreated retina (top) and Chronos-FP treated retina (bottom), using a comparable retinal eccentricity (between 3 and 12 mm from central retina) ( $p > 0.2$ , Kolmogorov-Smirnov test). (B) Histogram of ganglion cell firing rates from untreated retinas (top) and ChronosFP-expressing retinas (bottom); the two distributions were not statistically significantly different ( $p > 0.2$ , Kolmogorov-Smirnov test). Firing rates were measured in response to movies of natural scenes, including trees, landscapes, and people walking. All eyes were injected intravitreally with a ChronosFP vector 3–6 months before eye removal for electrophysiological recording. At the end of the recording, the presence of ChronosFP was verified by wavelength-selective activation of ganglion cells following pharmacological block of normal retinal signaling (Figure S1); i.e. the retinas responded to green light, which is ChronosFP-exciting, but not to red, which does not activate ChronosFP.

Briefly, the Luminance Dose Restriction in the 2014 ANSI takes into account studies by Morgan et al.<sup>59,60</sup> in nonhuman primates that showed retinal damage was occurring from exposures to 568 nm light at intensity levels below those reported in ANSI 2007. These experiments led to an addition to the damage spectrum. The damage spectrum of the Luminance Dose Restriction, denoted  $V(\lambda)$ , where  $\lambda$  is wavelength, peaks at 555 nm and decreases toward both ends of the visual spectrum (e.g.,  $V(555 \text{ nm}) = 1.0$ ,  $V(590 \text{ nm}) = 0.76$ ,  $V(500 \text{ nm}) = 0.32$ ). Yan et al.<sup>34</sup> provides software for other investigators in the field to assess any stimulation protocol with respect to the ANSI 2014 limits.

#### Current optogenetic clinical studies for RP using ganglion cells and bipolar cells as targets

Currently, there are four clinical trials using optogenetics as a potential therapy for RP (ClinicalTrial.gov identifier: NCT02556736, NCT03326336, NCT04278131, and NCT04945772). Among these, NCT02556736, NCT03326336, and NCT04278131 target retinal ganglion cells, and NCT04945772 targets ON bipolar cells. An advantage of targeting bipolar cells is the potential to utilize the remaining intrinsic retinal processing pathway. However, during retinal degeneration, the inner retina undergoes progressive remodeling,<sup>61</sup> which makes this strategy less suitable for patients with advanced disease.

For the studies targeting ganglion cells, several different optogenetic proteins are being used. The first clinical trial of an optogenetic therapy in humans (NCT02556736) began in 2015 using Chr2<sup>21</sup> as the optogenetic protein, based on the pioneering work of Zhuo-Hua Pan and his colleagues.<sup>7</sup> Two years later, another clinical trial

(NCT03326336) was started, using ChrimsonR (peak excitation: 590 nm), a red-shifted variant with faster kinetics,<sup>25</sup> producing some positive results in one subject.<sup>12</sup> Chronos has favorable qualities relative to Chrimson and Chr2 in both light sensitivity and kinetics: as shown in Klapoetke et al.,<sup>25</sup> it is 7-fold or more sensitive to light than Chrimson and more than 10-fold more sensitive than Chr2, according to the light levels required to achieve 100% spiking in cultured neurons<sup>25</sup>; the off-time of Chronos is 3.6 ms compared with Chr2 (~10 ms) and ChrimsonR (15.8 ms).<sup>25</sup> The faster off-time offers the ability to follow stimuli with rapid temporal variations, which is critical for devices delivering neurally coded visual input. With respect to light safety, while ChrimsonR was believed to have the highest margin of safety due to its red-shifted spectrum (peak excitation: 590 nm), this may no longer be the case, as indicated in ANSI 2014 (Luminance Dose Restriction in ANSI 2014) (see previous section about the updated damage spectrum from ANSI 2014, based on monkey studies).

#### Optogenetically activated PhNR-like responses in rd1 mice

In this paper, we referred to the ERG responses from Chronos-expressing retinas as “PhNR-like,” because the newly created wave comes from ganglion cells, as does the PhNR in WT animals.<sup>40</sup> Note, though, that we expect the Chronos-produced wave to be different from the WT-produced one, because the former is produced by direct activation of the ganglion cells, as opposed to the latter, which rides on waves of signals created by other cells in the retinal pathway. As a result, the Chronos-produced signal is expected to occur with a short latency, which is what was observed and shown in Figures 1 and 2. With respect to the amplitude of the response, it

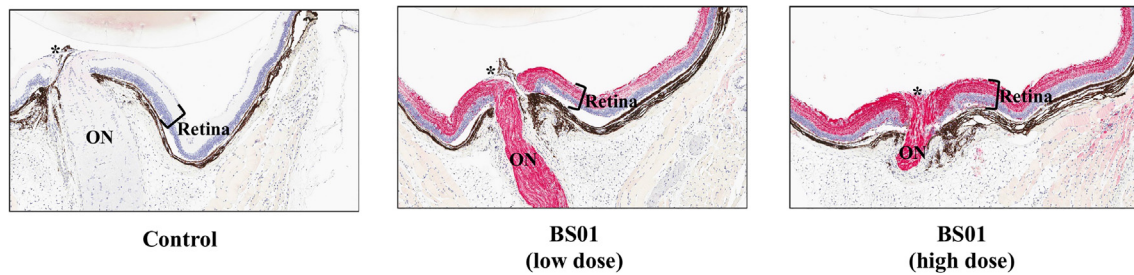


**Figure 8. Verification of BS01 expression in animals assessed for local tolerance**

Retinal sections of eyes from the 12-week euthanization of animals injected intravitreally with vehicle, BS01 at  $4.5 \times 10^8$  vg/eye (low dose), and BS01 at  $4 \times 10^9$  vg/eye (high dose) were stained with an antibody to GFP (magenta staining). All images were taken at  $\times 10$  magnification.

is difficult to predict how it should compare to the amplitude in the WT, but we do note that in mice treated with the highest vector dose used in this study (see Figure 2) the amplitude reached the same approximate level as is observed in WT PhNR ( $\sim 20 \mu\text{V}$  for the saturated response, Liu et al.<sup>62</sup>). Thus, in summary, while the BS01 treatment does not produce a completely normal PhNR, it does produce a significant ganglion cell response, which we referred to as “PhNR-like” and has the potential to provide visual signals to the brain and help visually impaired patients.

## MATERIALS AND METHODS

### Vector injections

All vectors were prepared in a balanced salt solution with 0.014% Tween 20 and delivered to the eye by intravitreal injection. For rodents, animals were anesthetized with intraperitoneal ketamine/xylazine (72 mg/kg ketamine and 4 mg/kg xylazine for mice, and 80 mg/kg ketamine and 10 mg/kg xylazine for rats), and the pupil was dilated with an atropine sulfate ophthalmic solution (1%). Using a Hamilton syringe under a dissecting microscope, the needle was passed through the sclera into the vitreous cavity. The injected volume was  $1 \mu\text{L}$  for mice and  $4 \mu\text{L}$  for rats. For nonhuman primates, animals were anesthetized with a mixture of ketamine/dexmedetomidine (5–10 mg/kg ketamine and 0.01–0.02 mg/kg dexmedetomidine) and then maintained with inhaled isoflurane/oxygen mixture. Pupils were dilated with 1% atropine sulfate, 2.5% phenylephrine hydrochloride, applied topically. The vector was injected intravitreally using a 3/10 mL U-100 insulin syringe with a 30-Gauge needle. The injected volume was 80–100  $\mu\text{L}$ . All animal experiments and procedures were performed according to the guidelines approved by the Institutional Animal Care and Use Committees.

### Electroretinography

For mice, animals were anesthetized with intraperitoneal ketamine/xylazine (72 mg/kg ketamine and 4 mg/kg xylazine), and the pupil was dilated with 1% atropine sulfate, 2.5% phenylephrine hydrochloride. To perform the ERG, a tungsten-wire electrode was placed on the corneal surface of the recorded eye and referenced to an electrode in the mouth. Visual stimuli were delivered with an LED stimulator with a 505-nm peak wavelength. The stimulator was placed 1.7 cm away from the cornea, subtending a visual angle of approximately

$100^\circ$ , with a peak intensity of  $0.06 \text{ mW}/\text{mm}^2$ . The stimulation was delivered as pulsed light, periodic at 10 Hz, pulse width at 11.2 ms. Data collection was carried out with the Espion E<sup>3</sup> ERG console (Diagnosys LLC, Lowell, MA).

Mouse model was rd1, which has rapid retinal degeneration. As shown in Nirenberg and Pandarinath,<sup>9</sup> photoreceptor outer segments disappear but the ganglion cell layer remains largely intact. The advantage to this model is that ERG responses recorded can be attributed to the transduced cells and not riding on signals passed from the photoreceptors.

For nonhuman primates, animals were anesthetized with a mixture of ketamine (5–10 mg/kg)/dexmedetomidine (0.01–0.02 mg/kg). Pupils were dilated with topical agents (1% atropine sulfate, 2.5% phenylephrine hydrochloride). To perform the ERG, a tungsten-wire electrode was placed on the corneal surface of the eye being tested, and referenced to a needle electrode placed in the scalp. Visual stimuli were delivered with a mini-ganzfeld stimulator placed close to the recorded eye. For the Naka-Rushton fit, photopic ERG stimulation was used following Joshi and colleagues<sup>53</sup>: 5-ms red light ganzfeld flashes ranging from  $0.00625$  to  $1.6 \text{ cd s}/\text{m}^2$  on a constant  $7 \text{ cd}/\text{m}^2$  blue background.

### Stimulation for light safety

Light stimulation was performed in 12 2- to 2.5-h sessions over a period of 6–8 weeks. The light was at an intensity of  $0.1 \text{ mW}/\text{mm}^2$  (a peak wavelength of 505 nm). The light was delivered in pulses with a pulse width of 5 ms, as it would be if neurally coded stimuli were used.<sup>9,34</sup> The stimulus subtending a visual angle of approximately  $60^\circ$  covered a large area of central retina, 4 mm diameter.<sup>34</sup> In each session, animals were anesthetized with isoflurane (99.9%) to a depth that minimized eye movements. Each animal was placed on its left side, with its right eye illuminated by the stimulus. The pupil was dilated with an atropine sulfate ophthalmic solution (1%) and the eye was kept wet with artificial tears applied regularly (every 7 min). The left eye was left untreated. Between sessions, the animals were exposed to normal room light with standard day/night cycles, as is standard in a rodent animal housing facility. Two to 4 weeks after the sessions were completed, the animals were euthanized and the retinas removed for examination.

### Histological analysis

For wholemount retinas, eyes were removed and fixed in 4% paraformaldehyde in PBS for 30 min. Retinas were dissected and fixed overnight in 4% paraformaldehyde. Autofluorescence was quenched with 1% sodium borohydride in PBS for 5 min. The retinas were permeabilized and blocked with 5% normal donkey serum (NDS), 1% bovine serum albumin (BSA) in PBS with 0.3% Triton X-100 for 1 h. The retinas were then labeled with rabbit anti-GFP Alexa Fluor 555 1:200 (Invitrogen-Molecular Probes, Life Technologies, Carlsbad, CA) overnight in 5% NDS, 1% BSA in PBS or with fluorescein peanut agglutinin (FITC PNA) 1:500 in 2% BSA (Vector Laboratories, Burlingame, CA) in PBS for 15 min. Then, the retinas were washed five times in PBS and incubated for 1.5 h at room temperature with the Alexa Fluor 647 donkey anti-goat immunoglobulin IgG 1:100 (Invitrogen-Molecular Probes, Life Technologies, Carlsbad, CA). The retinas were thoroughly washed in PBS and mounted.

When processed as sections, eyes were fixed in 4% paraformaldehyde. After 1 h, cornea and lens were removed without disturbing the retina. The retinas were further fixed for an additional 2–3 h at room temperature. The eyecups were rinsed with PBS and cryoprotected by 30% sucrose/PBS for 4 h at room temperature, then embedded in cryostat compound (Tissue TEK OCT, Sakura Finetek USA, Inc., Torrance, CA) and frozen at  $-80^{\circ}\text{C}$ . Retinas were sectioned perpendicularly from dorsal to ventral at 12- $\mu\text{m}$  thickness. For immunohistochemistry, retinal sections were rinsed in PBS and incubated in 0.3% Triton X-100 in PBS for 15 min, then blocked in 5% BSA in PBS for 1 h at room temperature. Sections were then incubated with anti-Brn3a (1:500, Santa Cruz, sc-31984) and anti-GFP (1:200 dilution, Life Technologies, A11122) at room temperature overnight. They were washed with PBS three times, followed by incubating with IgG secondary antibodies tagged with Alexa 594 and Alexa 488 (1:500 dilution, Molecular Probes, Eugene OR) at room temperature for 2 h, then washed with PBS. Sections were mounted with Vectashield Mounting Medium for Fluorescence (Vector Lab, H-10400, Burlingame, CA) and coverslipped.

### MEA recording

Electrophysiological recordings were obtained *in vitro* from isolated retinas. Briefly, the anterior portion of the eye and vitreous were removed immediately after enucleation, and the eyecup was placed in Ringer's solution and stored in darkness for at least 20 min before dissection. Under dim red light illumination, pieces of retina 1.5–3.0 mm in diameter were cut from central regions and placed onto a MEA for recording. The Ringer's solution was bubbled with 95%  $\text{O}_2$  and 5%  $\text{CO}_2$  and maintained at  $35\text{--}36^{\circ}\text{C}$ , pH 7.4. The stimulation and recording of retinal ganglion cells was performed as in Nirenberg and Pandarinath.<sup>9</sup> Spike waveforms were recorded using a Plexon Instruments Multichannel Neuronal Acquisition Processor (Dallas, TX). A standard spike sorting method was used to identify individual cells as in Nirenberg and Pandarinath.<sup>9</sup>

### Ocular toxicology assays

Before injections, an ocular examination was performed. If ocular findings were present, the animal was excluded from the study. Ocular examinations were also performed on weeks 2, 4, 8, and 12 post-injection by a licensed veterinary ophthalmologist. A slit lamp was used to assess anterior segments including cornea, iris, and lens. An indirect ophthalmoscope was used to assess the posterior segments including vitreous chambers and retinas. All observations were made in a masked fashion. There were two euthanization time points: week 4 and week 12. At scheduled necropsies, eyes of animals were collected in 4% paraformaldehyde. Following sufficient time in fixation, the tissues were trimmed, embedded in paraffin, sectioned, and stained with hematoxylin and eosin, and slides were examined. Immunohistochemical stains for GFP were also examined to verify the transgene expression.

### DATA AVAILABILITY

The authors declare that the data supporting the findings of this study are available within the paper and its [supplemental information](#) files. Otherwise, data generated and analyzed during the current study are available from the corresponding author on reasonable request.

### SUPPLEMENTAL INFORMATION

Supplemental information can be found online at <https://doi.org/10.1016/j.omtm.2023.05.005>.

### ACKNOWLEDGMENTS

We thank Vince Chiodo for helpful discussions about virus manufacture and for manufacturing the vectors at the early stages of this project. We thank Stephen Kaminsky and members of his lab for manufacturing the final versions of vector and for helping us prepare for an IND application. We thank Adrian Timmers for guiding and arranging the toxicology study. We thank Maksim Vakulenko, Nicola Corradi, Yunguo Yu, and Ping Zhu for their help with early animal studies. We thank Jonathan Victor for comments on the manuscript. The study was supported by a grant from Bionic Sight, Inc.

### AUTHOR CONTRIBUTIONS

B.Y., S.V., and S.N. performed and analyzed the electrophysiology experiments. W.-T.D. and B.Y. performed the non-GLP safety studies and K.E.C. performed the GLP safety studies. S.E.B. performed intravitreal injections. W.W.H. contributed to viral vector design and manufacture. S.N. designed the studies, and S.N. and B.Y. wrote the paper.

### DECLARATION OF INTERESTS

B.Y., W.W.H., and S.N. have financial interests in Bionic Sight, Inc. B.Y. is a consultant for Bionic Sight, Inc. S.N. is the principal and founder of Bionic Sight, Inc. W.W.H. is a cofounder of Bionic Sight, Inc.

### REFERENCES

1. Rayapudi, S., Schwartz, S.G., Wang, X., and Chavis, P. (2013). Vitamin A and fish oils for retinitis pigmentosa. *Cochrane Database Syst. Rev.* 2013, CD008428. <https://doi.org/10.1002/14651858.CD008428.pub2>.

2. Bainbridge, J.W.B., Mehat, M.S., Sundaram, V., Robbie, S.J., Barker, S.E., Ripamonti, C., Georgiadis, A., Mowat, F.M., Beattie, S.G., Gardner, P.J., et al. (2015). Long-term effect of gene therapy on Leber's congenital amaurosis. *N. Engl. J. Med.* 372, 1887–1897. <https://doi.org/10.1056/NEJMoa1414221>.
3. Jacobson, S.G., Cideciyan, A.V., Roman, A.J., Sumaroka, A., Schwartz, S.B., Heon, E., and Hauswirth, W.W. (2015). Improvement and decline in vision with gene therapy in childhood blindness. *N. Engl. J. Med.* 372, 1920–1926. <https://doi.org/10.1056/NEJMoa1412965>.
4. Bennett, J., Wellman, J., Marshall, K.A., McCague, S., Ashtari, M., DiStefano-Pappas, J., Elci, O.U., Chung, D.C., Sun, J., Wright, J.F., et al. (2016). Safety and durability of effect of contralateral-eye administration of AAV2 gene therapy in patients with childhood-onset blindness caused by RPE65 mutations: a follow-on phase 1 trial. *Lancet* 388, 661–672. [https://doi.org/10.1016/S0140-6736\(16\)30371-3](https://doi.org/10.1016/S0140-6736(16)30371-3).
5. Russell, S., Bennett, J., Wellman, J.A., Chung, D.C., Yu, Z.F., Tillman, A., Wittes, J., Pappas, J., Elci, O., McCague, S., et al. (2017). Efficacy and safety of voretigene neparovoc (AAV2-hRPE65v2) in patients with RPE65-mediated inherited retinal dystrophy: a randomised, controlled, open-label, phase 3 trial [published correction appears in *Lancet*. 2017 Aug 26;390(10097):848]. *Lancet* 390, 849–860. [https://doi.org/10.1016/S0140-6736\(17\)31868-8](https://doi.org/10.1016/S0140-6736(17)31868-8).
6. Maguire, A.M., Bennett, J., Aleman, E.M., Leroy, B.P., and Aleman, T.S. (2021). Clinical perspective: treating RPE65-associated retinal dystrophy. *Mol. Ther.* 29, 442–463. <https://doi.org/10.1016/j.ymthe.2020.11.029>.
7. Bi, A., Cui, J., Ma, Y.P., Olshevskaya, E., Pu, M., Dizhoor, A.M., and Pan, Z.H. (2006). Ectopic expression of a microbial-type rhodopsin restores visual responses in mice with photoreceptor degeneration. *Neuron* 50, 23–33. <https://doi.org/10.1016/j.neuron.2006.02.026>.
8. Tomita, H., Sugano, E., Yawo, H., Ishizuka, T., Isago, H., Narikawa, S., Kügler, S., and Tamai, M. (2007). Restoration of visual response in aged dystrophic RCS rats using AAV-mediated channelrhodopsin-2 gene transfer. *Invest. Ophthalmol. Vis. Sci.* 48, 3821–3826. <https://doi.org/10.1167/iovs.06-1501>.
9. Nirenberg, S., and Pandarinath, C. (2012). Retinal prosthetic strategy with the capacity to restore normal vision. *Proc. Natl. Acad. Sci. USA* 109, 15012–15017. <https://doi.org/10.1073/pnas.1207035109>.
10. Chaffiol, A., Caplette, R., Jaillard, C., Brazhnikova, E., Desrosiers, M., Dubus, E., Duhamel, L., Macé, E., Marre, O., Benoit, P., et al. (2017). A new promoter allows optogenetic vision restoration with enhanced sensitivity in macaque retina. *Mol. Ther.* 25, 2546–2560. <https://doi.org/10.1016/j.ymthe.2017.07.011>.
11. Gauvain, G., Akolkar, H., Chaffiol, A., Arcizet, F., Khoei, M.A., Desrosiers, M., Jaillard, C., Caplette, R., Marre, O., Bertin, S., et al. (2021). Optogenetic therapy: high spatiotemporal resolution and pattern discrimination compatible with vision restoration in non-human primates. *Commun. Biol.* 4, 125. <https://doi.org/10.1038/s42003-020-01594-w>.
12. Sahel, J.A., Boulanger-Scemama, E., Pagot, C., Arleo, A., Galluppi, F., Martel, J.N., Esposti, S.D., Delaux, A., de Saint Aubert, J.B., de Montleau, C., et al. (2021). Partial recovery of visual function in a blind patient after optogenetic therapy. *Nat. Med.* 27, 1223–1229. <https://doi.org/10.1038/s41591-021-01351-4>.
13. Lagali, P.S., Balya, D., Awatramani, G.B., Münch, T.A., Kim, D.S., Busskamp, V., Cepko, C.L., and Roska, B. (2008). Light-activated channels targeted to ON bipolar cells restore visual function in retinal degeneration. *Nat. Neurosci.* 11, 667–675. <https://doi.org/10.1038/nn.2117>.
14. Doroudchi, M.M., Greenberg, K.P., Liu, J., Silka, K.A., Boyden, E.S., Lockridge, J.A., Arman, A.C., Janani, R., Boye, S.E., Boye, S.L., et al. (2011). Virally delivered channelrhodopsin-2 safely and effectively restores visual function in multiple mouse models of blindness. *Mol. Ther.* 19, 1220–1229. <https://doi.org/10.1038/mt.2011.69>.
15. Macé, E., Caplette, R., Marre, O., Sengupta, A., Chaffiol, A., Barbe, P., Desrosiers, M., Bamberg, E., Sahel, J.A., Picaud, S., et al. (2015). Targeting channelrhodopsin-2 to ON-bipolar cells with vitreally administered AAV Restores ON and OFF visual responses in blind mice. *Mol. Ther.* 23, 7–16. <https://doi.org/10.1038/mt.2014.154>.
16. Batabyal, S., Gajjeraman, S., Pradhan, S., Bhattacharya, S., Wright, W., and Mohanty, S. (2021). Sensitization of ON-bipolar cells with ambient light activatable multi-characteristic opsin rescues vision in mice. *Gene Ther.* 28, 162–176. <https://doi.org/10.1038/s41434-020-00200->.
17. Barrett, J.M., Berlinguer-Palmini, R., and Degenaar, P. (2014). Optogenetic approaches to retinal prosthesis. *Vis. Neurosci.* 31, 345–354. <https://doi.org/10.1017/S0952523814000212>.
18. Galluppi, F., Pruneau, D., Chavas, J., Lagorce, X., Posch, C., Chenegros, G., Cordurié, G., Galle, C., Oddo, N., and Benosman, R. (2017). A stimulation platform for optogenetic and bionic vision restoration. In 2017 IEEE International Symposium on Circuits and Systems (ISCAS), pp. 1–4. <https://doi.org/10.1109/ISCAS.2017.8050683>.
19. Soltan, A., Barrett, J.M., Maaskant, P., Armstrong, N., Al-Atabany, W., Chaudet, L., Neil, M., Sernagor, E., and Degenaar, P. (2018). A head mounted device stimulator for optogenetic retinal prosthesis. *J. Neural. Eng.* 15, 065002. <https://doi.org/10.1088/1741-2552/aadd55>.
20. Mattis, J., Tye, K.M., Hyun, M., Fenko, L.E., Gradinaru, V., et al. (2011). Principles for applying optogenetic tools derived from direct comparative analysis of microbial opsins. *Nat. Methods* 9, 159–172. <https://doi.org/10.1038/nmeth.1808>.
21. Nagel, G., Szellas, T., Huhn, W., Kateriya, S., Adeishvili, N., Berthold, P., Ollig, D., Hegemann, P., and Bamberg, E. (2003). Channelrhodopsin-2, a directly light-gated cation-selective membrane channel. *Proc. Natl. Acad. Sci. USA* 100, 13940–13945. <https://doi.org/10.1073/pnas.1936192100>.
22. Kleinlogel, S., Feldbauer, K., Dempski, R.E., Fotis, H., Wood, P.G., Bamann, C., and Bamberg, E. (2011). Ultra light-sensitive and fast neuronal activation with the Ca<sup>2+</sup>-permeable channelrhodopsin CatCh. *Nat. Neurosci.* 14, 513–518. <https://doi.org/10.1038/nn.2776>.
23. Lin, J.Y., Knutsen, P.M., Muller, A., Kleinfeld, D., and Tsien, R.Y. (2013). ReaChR: a red-shifted variant of channelrhodopsin enables deep transcranial optogenetic excitation. *Nat. Neurosci.* 16, 1499–1508. <https://doi.org/10.1038/nn.3502>.
24. Chuong, A.S., Miri, M.L., Busskamp, V., Matthews, G.A.C., Acker, L.C., Sørensen, A.T., Young, A., Klapoetke, N.C., Henninger, M.A., Kodandaramaiah, S.B., et al. (2014). Noninvasive optical inhibition with a red-shifted microbial rhodopsin. *Nat. Neurosci.* 17, 1123–1129. <https://doi.org/10.1038/nn.3752>.
25. Klapoetke, N.C., Murata, Y., Kim, S.S., Pulver, S.R., Birdsey-Benson, A., Cho, Y.K., Morimoto, T.K., Chuong, A.S., Carpenter, E.J., Tian, Z., et al. (2014). Independent optical excitation of distinct neural populations [published correction appears in *Nat Methods*. 2014 Sep;11(9):971]. *Nat. Methods* 11, 338–346. <https://doi.org/10.1038/nmeth.2836>.
26. Gaub, B.M., Berry, M.H., Holt, A.E., Reiner, A., Kienzler, M.A., Dolgova, N., Nikonov, S., Aguirre, G.D., Beltran, W.A., Flannery, J.G., and Isacoff, E.Y. (2014). Restoration of visual function by expression of a light-gated mammalian ion channel in retinal ganglion cells or ON-bipolar cells. *Proc. Natl. Acad. Sci. USA* 111, E5574–E5583. <https://doi.org/10.1073/pnas.1414162111>.
27. Tochitsky, I., Kienzler, M.A., Isacoff, E., and Kramer, R.H. (2018). Restoring vision to the blind with chemical photoswitches. *Chem. Rev.* 118, 10748–10773. <https://doi.org/10.1021/acs.chemrev.7b00723>.
28. Berry, M.H., Holt, A., Broichhagen, J., Donthamsetti, P., Flannery, J.G., and Isacoff, E.Y. (2022). Photopharmacology for vision restoration. *Curr. Opin. Pharmacol.* 65, 102259. <https://doi.org/10.1016/j.coph.2022.102259>.
29. AbbVie. RST-001 phase I/II trial for advanced retinitis pigmentosa. <https://clinicaltrials.gov/ct2/show/NCT02556736>.
30. GenSight Biologics. Dose-escalation study to evaluate the safety and tolerability of GS030 in subjects with retinitis pigmentosa. <https://clinicaltrials.gov/ct2/show/NCT03326336>.
31. Nanoscope Therapeutics Inc. Efficacy and safety of vMCO-010 optogenetic therapy in adults with retinitis pigmentosa. <https://clinicaltrials.gov/ct2/show/NCT04945772>.
32. Bionic Sight Inc. BS01 in patients with retinitis pigmentosa. <https://clinicaltrials.gov/ct2/show/NCT04278131>.
33. The Laser Institute of America (2014). American National Standard for Safe Use of Lasers (ANSI 136.1-2014) (The Laser Institute of America).
34. Yan, B., Vakulenko, M., Min, S.H., Hauswirth, W.W., and Nirenberg, S. (2016). Maintaining ocular safety with light exposure, focusing on devices for optogenetic stimulation. *Vision Res.* 121, 57–71. <https://doi.org/10.1016/j.visres.2016.01.006>.

35. Farber, D., Flannery, J., and Bowes-Rickman, C. (1994). The rd mouse story: seventy years of research on an animal model of inherited retinal degeneration. *Prog. Retin. Eye Res.* *13*, 31–64.
36. Grimm, C., Wenzel, A., Stanescu, D., Samardzija, M., Hotop, S., Groszer, M., Naash, M., Gassmann, M., and Remé, C. (2004). Constitutive overexpression of human erythropoietin protects the mouse retina against induced but not inherited retinal degeneration. *J. Neurosci.* *24*, 5651–5658. <https://doi.org/10.1523/JNEUROSCI.1288-04.2004>.
37. Hackam, A.S., Strom, R., Liu, D., Qian, J., Wang, C., Otteson, D., Gunatilaka, T., Farkas, R.H., Chowers, I., Kageyama, M., et al. (2004). Identification of gene expression changes associated with the progression of retinal degeneration in the rd1 mouse. *Invest. Ophthalmol. Vis. Sci.* *45*, 2929–2942. <https://doi.org/10.1167/iovs.03-1184>.
38. Thyagarajan, S., van Wyk, M., Lehmann, K., Löwel, S., Feng, G., and Wässle, H. (2010). Visual function in mice with photoreceptor degeneration and transgenic expression of channelrhodopsin 2 in ganglion cells. *J. Neurosci.* *30*, 8745–8758. <https://doi.org/10.1523/JNEUROSCI.4417-09.2010>.
39. Pennesi, M.E., Michaels, K.V., Magee, S.S., Maricle, A., Davin, S.P., Garg, A.K., Gale, M.J., Tu, D.C., Wen, Y., Erker, L.R., and Francis, P.J. (2012). Long-term characterization of retinal degeneration in rd1 and rd10 mice using spectral domain optical coherence tomography. *Invest. Ophthalmol. Vis. Sci.* *53*, 4644–4656. <https://doi.org/10.1167/iovs.12-9611>.
40. Viswanathan, S., Frishman, L.J., Robson, J.G., Harwerth, R.S., and Smith, E.L., 3rd (1999). The photopic negative response of the macaque electroretinogram: reduction by experimental glaucoma. *Invest. Ophthalmol. Vis. Sci.* *40*, 1124–1136.
41. Nishiguchi, K.M., Carvalho, L.S., Rizzi, M., Powell, K., Holthaus, S.M.k., Azam, S.A., Duran, Y., Ribeiro, J., Luhmann, U.F.O., Bainbridge, J.W.B., et al. (2015). Gene therapy restores vision in rd1 mice after removal of a confounding mutation in Gpr179. *Nat. Commun.* *6*, 6006. <https://doi.org/10.1038/ncomms7006>.
42. Akkoyun, I., Karabay, G., Haberal, N., Dagdeviren, A., Yilmaz, G., Oto, S., Erkanli, L., and Akova, Y.A. (2012). Structural consequences after intravitreal bevacizumab injection without increasing apoptotic cell death in a retinopathy of prematurity mouse model. *Acta Ophthalmol.* *90*, 564–570. <https://doi.org/10.1111/j.1755-3768.2010.01963.x>.
43. Iwase, T., Fu, J., Yoshida, T., Muramatsu, D., Miki, A., Hashida, N., Lu, L., Oveson, B., Lima e Silva, R., Seidel, C., et al. (2013). Sustained delivery of a HIF-1 antagonist for ocular neovascularization. *J. Control. Release* *172*, 625–633. <https://doi.org/10.1016/j.jconrel.2013.10.008>.
44. Nomoto, H., Lavinsky, D., Paulus, Y.M., Leung, L.S., Dalal, R., Blumenkranz, M.S., and Palanker, D. (2013). Effect of intravitreal triamcinolone acetonide on healing of retinal photocoagulation lesions. *Retina* *33*, 63–70. <https://doi.org/10.1097/LAE.0b013e318261e34b>.
45. Applied Genetic Technologies Corp.. Safety and efficacy of rAAV-hRS1 in patients with X-linked retinoschisis (XLR5). <https://clinicaltrials.gov/ct2/show/NCT02416622>.
46. Finkelstein, D., Gouras, P., and Hoff, M. (1968). Human electroretinogram near the absolute threshold of vision. *Invest. Ophthalmol.* *7*, 214–218.
47. Martinez-Navarrete, G., Seiler, M.J., Aramant, R.B., Fernandez-Sanchez, L., Pinilla, I., and Cuenca, N. (2011). Retinal degeneration in two lines of transgenic S334ter rats. *Exp. Eye Res.* *92*, 227–237. <https://doi.org/10.1016/j.exer.2010.12.001>.
48. Onodera, H., Sasaki, S., Otake, S., Tomohiro, M., Shibuya, K., and Nomura, M. (2015). General considerations in ocular toxicity risk assessment from the toxicologists' viewpoints. *J. Toxicol. Sci.* *40*, 295–307. <https://doi.org/10.2131/jts.40.295>.
49. Nadal-Nicolás, F.M., Jiménez-López, M., Sobrado-Calvo, P., Nieto-López, L., Cánovas-Martínez, I., Salinas-Navarro, M., Vidal-Sanz, M., and Agudo, M. (2009). Brn3a as a marker of retinal ganglion cells: qualitative and quantitative time course studies in naive and optic nerve-injured retinas. *Invest. Ophthalmol. Vis. Sci.* *50*, 3860–3868. <https://doi.org/10.1167/iovs.08-3267>.
50. Elmore, S. (2007). Apoptosis: a review of programmed cell death. *Toxicol. Pathol.* *35*, 495–516. <https://doi.org/10.1080/01926230701320337>.
51. McGill, T.J., Prusky, G.T., Luna, G., LaVail, M.M., Fisher, S.K., and Lewis, G.P. (2012). Optomotor and immunohistochemical changes in the juvenile S334ter rat. *Exp. Eye Res.* *104*, 65–73. <https://doi.org/10.1016/j.exer.2012.09.006>.
52. Petrs-Silva, H., Dinculescu, A., Li, Q., Min, S.H., Chiodo, V., Pang, J.J., Zhong, L., Zolotukhin, S., Srivastava, A., Lewin, A.S., and Hauswirth, W.W. (2009). High-efficiency transduction of the mouse retina by tyrosine-mutant AAV serotype vectors. *Mol. Ther.* *17*, 463–471. <https://doi.org/10.1038/mt.2008.269>.
53. Joshi, N.R., Ly, E., and Viswanathan, S. (2017). Intensity response function of the photopic negative response (PhNR): effect of age and test-retest reliability. *Doc. Ophthalmol.* *135*, 1–16. <https://doi.org/10.1007/s10633-017-9591-0>.
54. Hawes, N.L., Smith, R.S., Chang, B., Davisson, M., Heckenlively, J.R., and John, S.W. (1999). Mouse fundus photography and angiography: a catalogue of normal and mutant phenotypes. *Mol. Vis.* *5*, 22.
55. Chang, B., Hawes, N.L., Hurd, R.E., Davisson, M.T., Nusinowitz, S., and Heckenlively, J.R. (2002). Retinal degeneration mutants in the mouse. *Vision Res.* *42*, 517–525. [https://doi.org/10.1016/s0042-6989\(01\)00146-8](https://doi.org/10.1016/s0042-6989(01)00146-8).
56. Timmers, A.M., Newmark, J.A., Turunen, H.T., Farivar, T., Liu, J., Song, C., Ye, G.J., Pennock, S., Gaskin, C., Knop, D.R., and Shearman, M.S. (2020). Ocular inflammatory response to intravitreal injection of adeno-associated virus vector: relative contribution of genome and capsid. *Hum. Gene Ther.* *31*, 80–89. <https://doi.org/10.1089/hum.2019.144>.
57. Simoncelli, E.P., and Olshausen, B.A. (2001). Natural image statistics and neural representation. *Annu. Rev. Neurosci.* *24*, 1193–1216. <https://doi.org/10.1146/annurev.neuro.24.1.1193>.
58. Olshausen, B.A., and Field, D.J. (2004). Sparse coding of sensory inputs. *Curr. Opin. Neurobiol.* *14*, 481–487.
59. Morgan, J.I.W., Hunter, J.J., Masella, B., Wolfe, R., Gray, D.C., Merigan, W.H., Delori, F.C., and Williams, D.R. (2008). Light-induced retinal changes observed with high-resolution autofluorescence imaging of the retinal pigment epithelium. *Invest. Ophthalmol. Vis. Sci.* *49*, 3715–3729. <https://doi.org/10.1167/iovs.07-1430>.
60. Morgan, J.I.W., Hunter, J.J., Merigan, W.H., and Williams, D.R. (2009). The reduction of retinal autofluorescence caused by light exposure. *Invest. Ophthalmol. Vis. Sci.* *50*, 6015–6022. <https://doi.org/10.1167/iovs.09-3643>.
61. Jones, B.W., Kondo, M., Terasaki, H., Lin, Y., McCall, M., and Marc, R.E. (2012). Retinal remodeling. *Jpn. J. Ophthalmol.* *56*, 289–306. <https://doi.org/10.1007/s10384-012-0147-2>.
62. Liu, Y., McDowell, C.M., Zhang, Z., Tebow, H.E., Wordinger, R.J., and Clark, A.F. (2014). Monitoring retinal morphologic and functional changes in mice following optic nerve crush. *Invest. Ophthalmol. Vis. Sci.* *55*, 3766–3774. <https://doi.org/10.1167/iovs.14-13895>.